

Profiling of hydrogen in metal-insulator-semiconductor sensors using neutron reflectivity

Steve T. Marshall,¹ Sushil K. Satija,² Bryan D. Vogt,³ and J. William Medlin^{1,a)}

¹University of Colorado at Boulder, Department of Chemical and Biological Engineering, Boulder, Colorado 80309, USA

²National Institute of Standards and Technology Center for Neutron Research, Gaithersburg, Maryland 20899, USA

³Arizona State University, Flexible Display Center, Tempe, Arizona 85284, USA

(Received 8 February 2008; accepted 14 March 2008; published online 15 April 2008)

Although interfacial hydrogen has long been accepted as the species responsible for H₂ detection in metal-insulator-semiconductor (MIS) sensors, direct observation of this species has been elusive. In this work, the use of neutron reflectivity (NR) to quantify the hydrogen concentration in regions of an MIS device is reported. The presence of multiple states at both the metal-insulator interface and within the insulator that may contribute to the hydrogen response is suggested by the scattering length density profiles obtained from NR. This technique provides a great promise for direct study of the detection mechanisms for MIS sensors. © 2008 American Institute of Physics.

[DOI: 10.1063/1.2908048]

The need for real-time detection of hydrogen and hydrogen-containing compounds is substantial in many fields, such as hydrogen leak detectors for hydrogen storage and fault gas sensors for precursors of electrical transformer explosions.¹ One potential tool for such detection is a metal-insulator-semiconductor (MIS) gas sensor. These devices consist of a thin layer of catalytic metal (such as palladium) and a layer of doped silicon separated by an insulator (such as silicon dioxide). This structure produces an “S” shaped capacitance-voltage curve. In the 1970s, Lundstrom *et al.* discovered that hydrogen can be incorporated into the device and produce a shift in the capacitance-voltage curve.² This shift has been observed over nearly 10 decades of hydrogen partial pressure, from the ultrahigh vacuum (UHV) range to the near atmospheric pressure range.³ Since this time, many theories have arisen regarding the cause of the shift. The most prevalent theory is that adsorbed hydrogen diffuses to the metal-insulator interface and forms dipoles;^{3,4} however, proof for such a mechanism lacks. The difficulty in directly detecting interfacial hydrogen raises a number of important questions, such as the following. What is the nature of the interfacial hydrogen site yielding response? How many sites are there? What is the effect of device structure on performance? Why do devices with different types of insulators behave differently?⁵

Experiments probing this mechanism have uncovered significant indirect evidence. In one class of experiments, hydrogen and deuterium are dosed to an oxygen precovered sensor in UHV and the desorption rate of the “HD” species is measured along with the sensor response. When all the oxygen is consumed, an immediate shift is noted in the sensor response along with an increase in HD desorption. By taking the difference between the hydrogen and deuterium adsorption rates and the HD desorption rate at the time of this shift, an estimation of the rate of adsorption of hydrogen and deuterium within the device can be estimated. With the use of microkinetic modeling, the interfacial coverage, and thus, to-

tal interfacial site concentration can be determined.^{6,7} While producing useful results, this technique only proves that hydrogen incorporation causes sensor response and not that the hydrogen induced response is situated at the metal-insulator interface. In another class of experiments, Eriksson and co-workers utilized the poor adhesion of Pd on SiO₂ to peel off the Pd film and perform atomic force microscopy on the Pd and SiO₂ sides of the interface. The observed morphology roughly correlated to sensor response.⁸ While this work produced valuable information, it also does not validate the above mechanism. Thus, there is a demonstrable need for a technique that can quantify hydrogen within the sensor as a function of depth.

Neutron reflectivity (NR) is a technique that meets this demand. In short, the sample is exposed to a beam of neutrons and the reflectivity is measured as a function of the momentum transfer q which is normal to the surface of the sensor

$$q = \frac{4\pi}{\lambda} \sin \theta, \quad (1)$$

where λ is the neutron wavelength (4.75 Å) and θ is the angle of reflection at the specular condition. The reflectivity of the film depends upon the distribution of the neutron scattering length density (NSLD) of the material through the film thickness. Since only momentum transfer in the z direction is probed, the NSLD profiles obtained from recursive fitting of the reflectivity data only provide the in-plane average NSLD. Unlike x rays where contrast proportionally varies to the electron density, neutron contrast is dependent on the specifics of the neutron interaction with the nucleus. This property results in a negative NSLD for H in comparison with positive NSLDs for Pd, SiO₂, and Si. The large difference in NSLD between H and other species in the MIS sensor provides significant contrast such that the hydrogen adsorption can be quantified via comparison of the sensor prior to and after H₂ exposure.

The sensor was prepared by depositing Pd on a commercially obtained Si wafer (3 in., n type, 1–100 Ω cm) with

^{a)}Electronic mail: will.medlin@colorado.edu.

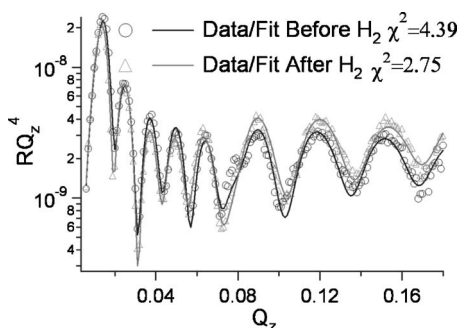


FIG. 1. Fits and reflectivity data before and after exposure to 0.1 torr hydrogen.

19 nm of thermally grown SiO₂ (Wafer World). The Pd deposition was performed using an electron beam evaporator (Angstrom Sciences) at Sandia National Laboratories in Livermore, CA. The sensor was then annealed in air at 400 °C for 1 h and exposed to 1000 ppm hydrogen in nitrogen for 2 h at room temperature. We previously observed that these preparation steps lead to a faster, more effective sensor. The sensor was placed in a stainless steel chamber, evacuated to 10⁻⁶ torr using a turbo pump, and characterized using the NG7 reflectometer at the National Institute of Standards and Technology (NIST) Center for Neutron Research. Scans were taken before and after saturation in 0.1 torr hydrogen.

The reflectivity data and associated fits are shown in Fig. 1. Shifts in the periodicity and amplitude upon H₂ exposure confirm the incorporation of hydrogen into the sensor. To quantify the change in hydrogen concentration, the data were fit using the Reflpack suite from NIST,⁹ which is based on a recursive NSLD box model with Gaussian smeared interfaces. High quality fits were obtained for the sensor structure before and after H₂ exposure. The scattering length density profiles from these fits are shown in Fig. 2. The profiles show distinct regions corresponding to the expected species present within the structure. The surface has a slightly negative NSLD which is consistent with mild hydrocarbon contamination. For the sensor in the absence of hydrogen, the NSLD increases due to the presence of the Pd to a plateau value which is consistent with bulk Pd. An increase, then a sharp decrease, followed by another increase in NSLD signify the interface between the Pd and the SiO₂. A low concentration of nickel contamination (equivalent to approxi-

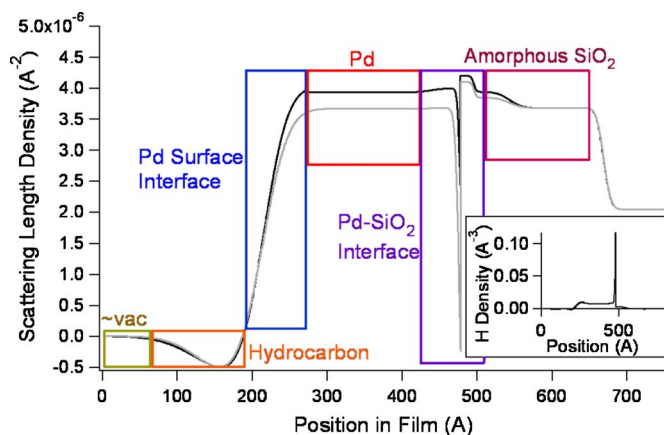


FIG. 2. (Color online) Scattering length density (SLD) profile derived from reflectivity fits. Inset: local hydrogen density derived from differences in SLD profiles before (black) and after (gray) exposure to 0.1 torr hydrogen.

mately 0.5 wt % on the Pd side and 8 wt % on the SiO₂ side of the interface) is a possible cause of this rise since Ni has a sufficiently large scattering length density ($9.4 \times 10^{-6} \text{ A}^{-2}$) (Ref. 10) to induce this effect and was previously used in the evaporator. The minimum in the NSLD is more intriguing. This minimum is likely a result of the fabrication process, either from residual H trapped at the interface, hydrocarbon contamination during metal deposition, or nanovoids developed from the H₂ preconditioning. We find that the data cannot be fit without this low NSLD at the interface. Next, the thermal oxide is encountered; this oxide layer exhibits three distinct densities. The highest NSLD is consistent with dense quartz, but amorphous SiO₂ has a lower physical density than quartz. Therefore, we suspect that this high NSLD is due to the diffusion of metal into the oxide layer. The NSLD then decreases over approximately 10 nm. Approximately one-half of the thermal oxide layer has a NSLD consistent with previous neutron studies.¹¹ Finally, the Si substrate is encountered.

The difference between the scattering length density profiles divided by the scattering length of H ($-3.74 \times 10^{-5} \text{ A}$) (Ref. 10) provides the H density as a function of position within the device, as shown in the inset of Fig. 2 (assuming negligible expansion from H incorporation). This analysis results in a coverage of $3.8 \times 10^{14} \text{ atoms/cm}^2$ at the Pd-SiO₂ interface and a total hydrogen quantity of $1.7 \times 10^{15} \text{ atoms/cm}^2$ within the SiO₂ phase. Note that the interface contains a much higher volumetric density of H than both the SiO₂ phase and the Pd bulk phase. The presence of hydrogen within the Pd is important since it is widely accepted that absorption into the Pd bulk only occurs after saturation of the sites causing the sensor response.^{6,7,12} Therefore, the H concentrations derived from the difference between these two profiles correspond to the maximum interfacial H concentration. This result indicates that neutron reflectivity can be used to detect H at different depths in the device and a significant accumulation occurs at the dielectric-Pd interface.

Previous work has speculated that hydrogen can absorb into the SiO₂ phase and bind to additional sensing sites, causing a well known “drift” effect which produces a larger and slower response in Pd-SiO₂-Si devices compared to devices with different dielectrics.^{13,14} In addition, deuterium atoms have been observed diffusing into the SiO₂ region of the Si-SiO₂-Si structure using the Rutherford backscattering,¹⁵ and it is widely accepted that hydrogen can diffuse into transistorlike structures and bind to defect sites at the SiO₂-Si interface.¹⁶ It is possible that the observed NSLD shift on the SiO₂ “side” of the interface after hydrogen introduction is the result of H absorption from the Pd into the SiO₂. However, this result could also be due to small quantities of contaminating metal in the SiO₂ providing sites for H binding. Further studies of the H density profiles in different film structures are necessary to more clearly identify the binding sites in the interfacial region.

To gain a more complete picture of sensor behavior, these results were correlated to the sensor response. The sample was diced into $\sim 1/8$ in. square pieces and three segments from different sections of the wafer were separately placed into a flow cell device capable of simultaneously measuring the inflection point of the capacitance-voltage curve and dosing known concentrations of hydrogen, nitrogen, and oxygen. The details of this system are described

elsewhere.¹ The sensor was exposed to a low flow of ultra-high purity hydrogen at room temperature to simulate the saturation conditions observed in the reflectivity experiments. After equilibration, oxygen was introduced to speed response back to the initial state through the highly exothermic water formation reaction. In all cases, the wafer segments returned to their original response prior hydrogen addition. The experiments yielded an average response under saturation of 580 ± 110 mV.

Using these data and the results of the reflectivity work, the average dipole moment of adsorbed H can be calculated by using the commonly accepted equation^{6,7,10} (where ΔV is the change in voltage, n_i is the number of adsorbed H atoms per unit area, d is the dipole moment, and ϵ is the permittivity of vacuum)

$$\Delta V = \frac{n_i d}{\epsilon}. \quad (2)$$

Using the change in voltage found in the sensor response experiment, the number of adsorbed H atoms found through the reflectivity experiments, and the permittivity of vacuum the dipole moment of H is calculated to be 0.41 ± 0.08 D only assuming the interfacial H contributes to the response and 0.09 ± 0.08 D assuming all H within the sensor excluding the bulk Pd contributes to the response. The small associated dipole moment of the latter calculation compared to the dipole moments of an OH radical (1.7 D) and a SiH radical (0.3 D)¹⁷ strongly suggests either the response is entirely due to H at the Pd–SiO₂ interface or multiple states within the device have different dipole moments. The estimated dipole moment of 0.41 D only considering interfacial H is much larger than moments typically associated with Pd surfaces (0.02–0.07 D),^{7,2,18} indicating an important and perhaps dominant role of the oxide in the H binding site.

The average dipole moments are smaller than the results reported in previous experiments. Initial studies utilizing the H₂/D₂ mixture method (described above) suggested a dipole moment of nearly 2 D.⁷ Subsequent improvements in the experimental procedure yielded an estimated dipole moment of 0.6–0.7 D,⁶ more in line with our estimated 0.41 D value only considering interfacial H. Inconsistency in reported values may be due to different preparation methods which affect film morphologies and impurities present within prepared films and silicon/oxide substrates. Since NR can directly quantify hydrogen content and provide structural details (and can provide indications as to the identity of impurities), it

represents an excellent method for future study of the source of variability between devices.

Overall, this work demonstrates the viability of neutron reflectivity for studying hydrogen accumulation in MIS sensors. To gain deeper understanding of these devices and better correlate response to absorbed hydrogen, additional NR experiments must be conducted under different hydrogen pressures, at different temperatures, and with varied gate metals and insulators.

S.T.M. acknowledges support from a Graduate Assistantship in Areas of National Need from the U.S. Department of Education. We acknowledge the National Institute of Standards and Technology, U.S. Department of Commerce, in providing the neutron research facilities used in this work. We also acknowledge the Electric Power Research Institute (EPRI) for funding this work and assistance from Robert Bastasz and Josh Whaley at Sandia National Laboratories in Livermore, CA with device fabrication.

¹D. Li, A. H. McDaniel, R. Bastasz, and J. W. Medlin, *Sens. Actuators B* **115**, 86 (2006).

²I. Lundstrom, M. S. Shivaraman, and C. M. Svensson, *J. Appl. Phys.* **46**, 3876 (1975).

³L. G. Ekedahl, M. Eriksson, and I. Lundstrom, *Acc. Chem. Res.* **31**, 249 (1998).

⁴J. W. Medlin, in *Encyclopedia of Sensors*, edited by C. A. Grimes, E. C. Dickey, and M. V. Pishko (American Scientific Publishers, California, 2005).

⁵M. Eriksson, A. Salomonsson, I. Lundstrom, D. Briand, and A. E. Abom, *J. Appl. Phys.* **98**, 034903 (2005).

⁶A. Salomonsson, M. Eriksson, and H. Dannetun, *J. Appl. Phys.* **98**, 014505 (2005).

⁷J. Fogelberg, M. Eriksson, H. Dannetun, and L. G. Petersson, *J. Appl. Phys.* **78**, 988 (1995).

⁸A. E. Abom, R. T. Haasch, N. Hellgren, N. Finnegan, L. Hultman, and M. Eriksson, *J. Appl. Phys.* **93**, 9760 (2003).

⁹P. A. Kienziele, K. V. O'Donovan, J. F. Ankner, N. F. Berk, and C. F. Majkrzak, see <http://www.ncnr.nist.gov/reflpak>

¹⁰J. W. Medlin, A. E. Lutz, R. Bastasz, and A. H. McDaniel, *Sens. Actuators B* **96**, 290 (2003).

¹¹A. Munter, Scattering Length Density Calculator, see <http://www.ncnr.nist.gov/resources/sldcalc.html>

¹²V. Bertagna, R. Erre, M. L. Saboungi, S. Petitdidier, D. Levy, and A. Menelle, *Appl. Phys. Lett.* **84**, 3816 (2004).

¹³I. Robins, *Sens. Actuators B* **15–16**, 238 (1993).

¹⁴M. Armgarth and C. Nylander, *Appl. Phys. Lett.* **39**, 91 (1981).

¹⁵S. M. Myers, G. A. Brown, A. G. Revesz, and H. L. Hughes, *J. Appl. Phys.* **73**, 2196 (1993).

¹⁶S. M. Myers and P. M. Richards, *J. Appl. Phys.* **67**, 4064 (1990).

¹⁷R. D. Johnson, III, NIST Computational Chemistry Comparison and Benchmark Database, NIST Standard Reference Database Number 101 Release 14; see <http://srdata.nist.gov/cccbdb>

¹⁸K. Christmann, *Surf. Sci. Rep.* **9**, 1 (1988).